Finite-size scaling for quantum criticality using the finite-element method

Edwin Antillon,[1] Birgit Wehefritz-Kaufmann,[1,2] and Sabre Kais[1,3,*]

[1]*Department of Physics, Purdue University, West Lafayette, Indiana 47907, USA*
[2]*Departments of Mathematics and Physics, Purdue University, West Lafayette, Indiana 47907, USA*
[3]*Department of Chemistry, Purdue University, West Lafayette, Indiana 47907, USA*

Finite size scaling for the Schrödinger equation is a systematic approach to calculate the quantum critical parameters for a given Hamiltonian. This approach has been shown to give very accurate results for critical parameters by using a systematic expansion with global basis-type functions. Recently, the finite-element method was shown to be a powerful numerical method for *ab initio* electronic-structure calculations with a variable real-space resolution. In this work, we demonstrate how to obtain quantum critical parameters by combining the finite-element method (FEM) with finite size scaling (FSS) using different *ab initio* approximations and exact formulations. The critical parameters could be atomic nuclear charges, internuclear distances, electron density, disorder, lattice structure, and external fields for stability of atomic, molecular systems and quantum phase transitions of extended systems. To illustrate the effectiveness of this approach we provide detailed calculations of applying FEM to approximate solutions for the two-electron atom with varying nuclear charge; these include Hartree-Fock, local density approximation, and an "exact" formulation using FEM. We then use the FSS approach to determine its critical nuclear charge for stability; here, the size of the system is related to the number of elements used in the calculations. Results prove to be in good agreement with previous Slater-basis set calculations and demonstrate that it is possible to combine finite size scaling with the finite-element method by using *ab initio* calculations to obtain quantum critical parameters. The combined approach provides a promising first-principles approach to describe quantum phase transitions for materials and extended systems.

PACS number(s): 02.70.Dh, 64.60.an, 05.70.Jk, 82.60.−s

I. INTRODUCTION

The theory of finite size scaling (FSS) in statistical mechanics can provide us with numerical methods [1–8] capable of obtaining accurate results for infinite systems by studying the corresponding small systems. In the past, basis set approximation to many-body systems have been combined with FSS to obtain critical parameters, where calculations for these systems were done by expanding the wave function in Slater-type basis sets or Gaussian-type basis functions. However, a generalization of larger atomic and molecular systems proved itself difficult using these types of functions [9,10].

More recently, we have combined FSS with the finite-element method (FEM) in order to obtain critical parameters in a potential that admits a finite number of bound states and we obtained excellent results by using both finite-element and Slater-type basis functions [11]. For this potential we also established that the finite-difference (FD) method can be combined with FSS. The FD method, however, is not a variational method since it approximates the operators (i.e., the derivative) and therefore can result in errors of either sign [12]. As a result, we observed nonmonotonic behavior of the calculated critical parameters with respect to the number (N) of grid points used [13]. Nevertheless, for a large-enough number of grid points N one can recover the correct asymptotic behavior in the large N limit. For this particular example we used FD to fourth order and in FEM we used C^1-continuous basis.

In this paper, we present a method to combine FEM with FSS for electronic-structure calculations near regions of criticality. We note that *any* method where the wave function can be expanded in a complete basis (or set of grid points) should also work, provided that in the infinite basis limit ($N \to \infty$) it becomes arbitrarily close to the the exact wave function. The main advantage of FEMs, over other global basis methods, resides in the fact that matrices obtained by these numerical methods are often banded and tend to be sparse since variables are not coupled over arbitrarily large distances. This is ideal for describing extended systems since it facilitates parallelization [14]. Moreover, due to the polynomial nature of the basis set most integrals involved can be evaluated easily and accurately with a better convergence with respect to the basis set size.

We examine the two-electron system with different levels of approximations to the ground state energy, by solving the system using FEM both *exactly* and using *mean-field equations* and demonstrate that this formalism is general and that it has potential for more complex systems by solving Hartree-Fock equations or Kohn-Sham equations in density-functional theory. The paper is organized as follows: In Sec. II we discuss FEM formalism, in Sec. III we discuss the FSS approach to quantum systems, in Secs. III and IV we combine FSS with FEM to compute calculations of critical parameters for two-electron atoms, and, lastly, in Sec. V we discuss the results and applications to extended systems.

II. FINITE-ELEMENT METHOD IN ELECTRONIC-STRUCTURE CALCULATIONS

Computational methods in quantum chemistry typically make use of Slater or Gaussian basis sets to approximate solutions in atomic or molecular systems. The advantages

*kais@purdue.edu

of these methods are that some of the integrals involved in the calculations are analytical and very accurate results can be obtained for these integrals. However, there are problems in extrapolating to the complete basis limit. Plane wave methods, having a complete basis, present some difficulties if nonperiodic boundary conditions are to be used such as in molecule calculations. A common trait of all these methods is that they employ global basis, which can result in some difficulties for the formulation of large problems. First, the matrix formulation becomes dense using global basis and therefore ill-conditioned for parallelism [14]. While for some complex objects, convergence issues may arise if there are large variations of potential terms in small regions which cannot be captured by the traditional Gaussian basis set that are centered on the nuclei.

The FEM presents an alternative solution to these problems. This method uses a variational method to solve differential equations by discretizing a continuous solution to a set of values in subdomains, called elements, and employs a *local* basis expansion in terms of polynomials with variable real-space resolution, allowing for convergence to be controlled systematically. The locality of the bases in real-space results in sparse and banded matrices, where the number of operations for matrix-vector multiplication can be reduced from $O(\mathbf{N} \log \mathbf{N})$ for dense matrices to $O(\mathbf{N})$ for sparse matrices, where $\mathbf{N}$ is the dimension of the matrix [14]. Some of the first applications of FEM in engineering date back to 1950, in problems such as elasticity and structural analysis in civil engineering and aeronautical engineering, respectively. In the 1970s, some applications to quantum mechanical problems appeared, but were limited to small systems due to the storage limitation [15,16]. Recently, advances in high-performance computing make FEM a viable alternative to the traditional approaches of electronic-structure calculations [17,18]. The sparsity of the global matrices resulting from the FEM makes the parallel formulation more affordable. Alizadean *et al*. have recently applied a *divide-and-conquer* method to the FEM-Hartree-Fock approach for electronic calculations showing a facilitation on parallelization and reduced scaling for larger systems [19].

We briefly describe the FEM formulation for a given Hamiltonian to be used in later sections. Let us consider the following one-particle Hamiltonian:

$$-\frac{1}{2}\nabla^2 \Psi_i + V \Psi_i = \epsilon_i \Psi_i,   \quad (1)$$

where ϵ_i and Ψ_i are the energy eigenvalue and eigenvector, respectively, and V is an arbitrary potential that will represent a sum of terms such as the electron-nuclear potential (V_{en}), Hartree potential (V_H), and exchange-correlation potentials (V_{xc}). We can reformulate this problem into a *weak form* by taking an inner product of an arbitrary "*test* function" Φ with Eq. (1):

$$\int_\Omega \Phi \left[-\frac{1}{2}\nabla^2 + V - \epsilon_i \right] \Psi_i d\Omega = 0.   \quad (2)$$

This relaxes the problem into a variational form where instead of finding an exact solution in the domain Ω, we find a solution that satisfies Eq. (1) in an average sense everywhere. We then arrive at an equivalent equation by integrating by parts (in real space)

$$\int_\Omega \frac{1}{2}\nabla\Phi(r) \cdot \nabla\Psi_i(r)d\Omega - \int_\Gamma \frac{1}{2}\Phi(r)\nabla\Psi_i(r) \cdot \hat{n}d\Gamma$$
$$+ \int_\Omega \Phi(r)(V - \epsilon_i)\Psi_i(r)d\Omega = 0,   \quad (3)$$

where Γ is a boundary term and $\hat{n}$ is the outward unit normal at **r**. In the absence of external fluxes we can employ Neumann boundary conditions $[\nabla\Psi_i(r) \cdot \hat{n} = f(r)r \in \Gamma]$. Furthermore, in radial coordinates ($d\Omega = r^2 dr$) we can write the surface term in the following form:

$$\int_\Gamma \frac{1}{2}\Phi(r)\nabla\Psi_i(r) \cdot \hat{n}d\Gamma = \left[\frac{1}{2}\Phi(r)f(r)r^2 \right]_0^{r_{cut}}.   \quad (4)$$

This surface term vanishes trivially at $r = 0$, while for $r = r_c$, it can be removed if we choose a test function $\Phi(r)$ that vanishes at $r = r_{cut}$. Since Eq. (3) is satisfied for any $\Phi(r)$, we can choose $\Phi = \Psi^*$ and in this manner it reduces the problem to an eigenvalue problem. The wave function $\Psi_i(r)$ can be then discretized using the *Garlekin* approximation [15,16]:

$$|\Psi(r)\rangle \approx \mathbf{N^T}|\psi\rangle = \sum_i N_i(r)|\psi_i\rangle,   \quad (5)$$

where $N_i(r)$ are piecewise-linear C^0-continuous functions (i.e., continuous but not necessarily smooth) and $|\psi_i\rangle$ are the nodal degrees of freedom. Smoother bases can be constructed by using higher order polynomial (C^n continuous, $n \geqslant 1$) and by extending the nodal space to include the derivative of the wave function at the node, viz., $|\Psi\rangle = \sum_i N_i(r)|\psi_i\rangle + \partial_x N_i(r)|\partial_x\psi_i\rangle$; this ensues continuity of the wave function between the nodes. In the nodal basis, the generalized eigenvalue problem reads

$$\sum_{ij}\langle\psi_i|H_{ij}|\psi_j\rangle = \epsilon \sum_{ij}\langle\psi_i|S_{ij}|\psi_j\rangle,   \quad (6)$$

where the above terms can be written in terms of local basis representation, viz.,

$$H_{ij} = \int_\Omega \left[\frac{1}{2}\nabla N_i \cdot \nabla N_j^T + V N_i N_j^T \right]d\Omega,$$
$$S_{ij} = \int_\Omega N_i N_j^T d\Omega.$$

The FEM takes advantage of the strict locality of its basis to yield matrices that are sparse and structured and due to the polynomial nature of the basis most integrals can be easily evaluated, as in global basis approaches. Moreover, since the method is variational, all errors are of the same sign, leading to monotonic convergence often from below [20].

III. FINITE SIZE SCALING

We now discuss the role of FSS in systems exhibiting critical behavior. Phase transitions are associated with singularities of the free energy that occur only in the thermodynamic limit [21,22]. Near criticality, fluctuations in the system become correlated over distances of the order of the correlation length ξ, while for second order phase transitions, this correlation length ξ diverges.

The theory of FSS can be used to extract universal parameters describing the transition by studying systems of finite size [1,2,4–8]. Any physical quantity (P) that would diverge in the thermodynamic limit, becomes now "rounded off" in the finite systems (of size L) by a scaling function $f(x)$ [1,2],

$$\frac{P_L(t)}{P_\infty} = f\left(\frac{L}{\xi_\infty(t)}\right), \qquad (7)$$

where $t = (T - T_c)/T_c$ is a reduced critical parameter describing the phase transition and ξ_∞ is the correlation length of the system in the thermodynamic limit.

While classical phase transitions are governed by the fluctuation of temperatures that tend to minimize the free energy, at zero temperature, these fluctuations are driven by Heisenberg's *uncertainty principle* [23]. A signature of a phase transition is *nonanalyticity* of the ground state energy $E(\lambda)$ with respect to a parameter λ in the Hamiltonian. The nonanalyticity can be the result of avoided crossing or actual level crossing. In the first case, the configuration of the system that minimizes the energy maintains the energy gap (ΔE_λ) between the first excited energy state and the ground state as the parameter λ is varied. In the latter case, the energy levels cross so that the energy is now minimized by a configuration that previously corresponded to the first excited state of the system.

To pin down the transition point involves computing the energy accurately near the critical point. However, this can be quite a challenge since most real systems lack an analytical solution to the ground state energy and approximation methods, such as perturbation theory or mean-field methods (Hartree-Fock, DFT), which are viable options in stable systems, in general are not well defined, or become ill-conditioned near critical points.

This is where the theory of FSS can be recast in the context of the Hilbert space. Any given approximation to the ground state energy will result in a "rounding" effect from the "true" critical behavior, since any approximation to a wave function can be expanded in some basis and truncated to some order N; that is,

$$|\Psi\rangle = \sum_i^N a_i |\phi_i\rangle. \qquad (8)$$

FSS has been used in quantum systems [24–33]. In this approach, the finite size corresponds not to the *spatial* dimension but to the *number of elements* (**N**) in a complete basis set used to expand the exact eigenfunction of a given Hamiltonian [34–38]. In the variational approach singularities in different mean values will occur only in the limit of infinite number basis function, viz.,

$$\langle O \rangle_\lambda^\infty \sim (\lambda - \lambda_c)^{\mu_o}. \qquad (9)$$

The FSS *ansatz* in the Hilbert space takes the following form (for expectation values of operators acting on the Hilbert space). There is a scaling function $F(x)$ such that

$$\langle O \rangle_\lambda^{(N)} \sim \langle O \rangle_\lambda^\infty F_O(N|\lambda - \lambda_c|^\nu), \qquad (10)$$

where λ is a critical parameter in the Hamiltonian, O is a quantum mechanical operator near criticality, and F_O is a scaling function for each different operator but with a unique scaling exponent. At the critical point, the expectation value is related to N as a power law, $\langle O \rangle^{(N)} \sim N^{-\mu_o/\nu}$. In this manner the scaling function F_O will remove the divergence as it is computed in the finite basis.

The asymptotic behavior of operators near the critical point, in this case the ground state energy, can be expressed using critical exponents similarly to classical phase transitions, viz.

$$\Delta E_\lambda \sim (\lambda - \lambda_c)^\alpha, \qquad (11)$$

where α is a universal critical exponent. In addition to the vanishing energy scale, a diverging length scale also occurs which is associated with the exponential decay of equal-time correlations in the ground state of the system [23]. For our case, we focus on the behavior of the wave function at threshold, where the correlation length is defined by

$$\xi \sim |\lambda - \lambda_c|^{-\nu}. \qquad (12)$$

In order to apply FSS method to quantum system, we assume a Hamiltonian of the form

$$H = H_o + V_\lambda, \qquad (13)$$

where λ is the coupling parameter showing a phase transition at $\lambda = \lambda_c$. For potentials linear in $\lambda (V_\lambda = \lambda V)$, Simon [39] showed that the critical exponent is equal to one if and only if the Hamiltonian $H(\lambda_c)$ has a normalizable eigenfunction with eigenvalue equal to zero. The existence or absence of a bound state at the critical point is related to the type of singularity in the energy. Using statistical mechanics terminology, we can associate a "first order phase transition" with the existence of a normalizable eigenfunction at the critical point. The absence of such a function could be related to a "continuous phase transition." To obtain the critical parameters, we define the following function that will remove the N-dependence at a critical point:

$$\triangle_O(\lambda; N, N') = \frac{\ln\left(\langle O \rangle_\lambda^N / \langle O \rangle_\lambda^{N'}\right)}{\ln(N'/N)}. \qquad (14)$$

For the energy operator $O = H$, and using the customary α Greek letter for the corresponding exponent μ_o we have

$$\triangle_H(\lambda_c; N, N') = \frac{\alpha}{\nu}. \qquad (15)$$

To arrive at an expression that isolates the critical exponent α from numerical calculations, we make use of the *Hellmann-Feynman* theorem [40],

$$\frac{dE_\lambda}{d\lambda} = \left\langle \frac{dH_\lambda}{d\lambda} \right\rangle. \qquad (16)$$

At this point it becomes convenient to define another function that will be used in the following sections:

$$\Gamma_\alpha(\lambda, N, N') = \frac{\triangle_H(\lambda; N, N')}{\triangle_H(\lambda; N, N') - \triangle_{\frac{\partial H_\lambda}{\partial \lambda}}(\lambda; N, N')}. \qquad (17)$$

At the critical point this function is independent of N and N' and takes the value of α. Namely, for $\lambda = \lambda_c$ and any values of N and N' we have

$$\Gamma_\alpha(\lambda_c, N, N') = \alpha. \qquad (18)$$

IV. IMPLEMENTATION

In the following, we illustrate the combined approach (FEM + FSS) for the two-electron atom, but emphasize that the method is general and can be applied to more complex atomic and molecular systems. We seek the minimum charge (*critical charge*) needed to bind both electrons to the nucleus with charge Z. It is well known that ignoring the electron-electron energy correlation will not predict the stability of H^- [41], since the *critical charge* obtained by such assumption is $Z_c \approx 1.02$. Stillinger (1974) [42] took into account the *e-e* correlation by using a nonlinear wave function $e^{-ar_1-br_2} + e^{-ar_1-br_2}$ in order to find the minimum energy as the nuclear charge Z was varied. He found a critical charge around $Z_c \approx 0.9537$. Baker *et al.* [43] performed a thorough 401-order perturbation calculation to resolve the controversy for the critical charge; they obtained a critical charge of $Z_c \approx 0.911\,03$. This is the value we use as reference. In the following sections we illustrate the mean-field equations and exact formulations for the ground state of the two-electron system, while in the next section we apply FSS to these approximations. Let us start with the Hamiltonian for the two-electron atoms; it is given by

$$H = -\frac{1}{2}\nabla_1^2 - \frac{1}{2}\nabla_2^2 + \frac{e^2}{|r_1 - r_2|} - \left(\frac{Z}{r_1} + \frac{Z}{r_2}\right), \quad (19)$$

where r_1 and r_2 are the coordinates of the two electrons referenced from the nuclei. We use hartree units ($\hbar = m = e = 1$) throughout in our calculations.

A. Hartree-Fock (HF) approximation

In the Hartree approximation the total wave function is approximated as a product of single particle wave functions is $\Psi(r_1, r_2) = \psi_1(r_1)\psi_2(r_2)$. We can arrive at a self-consistent

form by multiplying the Hamiltonian by the complex conjugate of the aforementioned wave function and integrating one coordinate out, we arrive at

$$\left[-\frac{1}{2}\nabla_1^2 - \frac{Z}{r_1} + \int d^3r_2 \frac{1}{|r_1 - r_2|}|\psi_2(r_2)|^2\right]\psi_1(r_1) = \epsilon\psi_1(r_1). \quad (20)$$

Using the FEM (see Sec. II) this expression can be reduced to a generalized eigenvalue problem $H_{kl}\psi_l = \epsilon S_{kl}\psi_l$. The Hamiltonian H_{kl} is written in terms of the single electron energy term h_{kl} (i.e., $-\frac{1}{2}\nabla^2 - \frac{Z}{r}$) and a *direct* Coulomb term J_{kl} defined below, viz.,

$$H_{kl} = \int\left[\overbrace{\frac{1}{2}\nabla N_k * \nabla N_l^T + \frac{1}{r}N_k N_l^T}^{h_{kl}} + \overbrace{\sum_{ij} Q_{klij}\psi_i\psi_j}^{J_{kl}}\right]d^3r_1, \quad (21)$$

$$Q_{klij} \equiv N_k(r_1)^* N_l(r_1)\int \frac{1}{|r_1 - r_2|}N_i(r_2)^* N_j(r_2)d^3r_2,$$

$$S_{kl} = \int N_k N_l^T d^3r_1.$$

Since electrons are fermions, the product of the single particle states needs to be antisymmetric with respect to exchange of the coordinates on the electrons. This can be achieved by writing the wave function as a Slater determinant [44]:

$$\Psi(r_1, r_2) = \begin{vmatrix} \psi_1(r_1) & \psi_2(r_1) \\ \psi_1(r_2) & \psi_2(r_2) \end{vmatrix}. \quad (22)$$

Searching for the best Slater determinant self-consistently in the Hamiltonian [Eq. (19)] leads to the Hatree-Fock equations [44–46]

$$\int \psi_1^*(r_1)\left(-\frac{1}{2}\nabla_1^2 - \frac{Z}{r_1} - \epsilon\right)\psi_1(r_1)d^3r_1 + \frac{1}{2}\iint\left\{|\psi_1(r_1)|^2\frac{1}{|r_1-r_2|}|\psi_2(r_2)|^2 - \psi_1^*(r_2)\psi_2^*(r_2)\frac{1}{|r_1-r_2|}\psi_1(r_1)\psi_2(r_1)\right\}d^3r_1 d^3r_2 = 0, \quad (23)$$

where the additional term on the right is known as the *exchange Coulomb term*, denoted by K_{kl}, and tends to repel states of the same (parallel) spin. We can write this term in the local basis form by looking at the direct Coulomb term and noting that the indices $(i, j) \in \psi_2$ and similarly indices $(k, l) \in \psi_1$. The operator K_{kl} is obtained from J_{kl} by switching indices $(j \leftrightarrow l)$, which effectively switches the coordinates r_1 and r_2 on two of the wave functions and makes this operator nonlocal.

The ground state energy (for N_e electrons) is determined by solving for the ground state eigenfunction $|\psi_g\rangle$ for the eigenvalue problem [Eq. (23)] and computing the expectation value below (to avoid double counting terms),

$$E_{HF} = \sum_j^{N_e}\langle\psi_g|h_j - \frac{1}{2}(J_j - K_j)|\psi_g\rangle. \quad (24)$$

Note that, for our case, the exchange term does not arise since the ground state of the helium atom does not have parallel spins. In order to improve upon the HF approximation we can take into account the correlation energy from an approximation to the free electron gas due to Wigner. Here the "correlation" potential can be obtained from Refs. [47,48]. Note that the references cited use rydberg units, and reference [47] additionally uses $e^2 = 2, \hbar/2m = 1$. In hartrees the correlation potential is given by

$$V_c(r) = \frac{0.29}{5.1 + r_s(r)}, \quad (25)$$

where r_s is the local density parameter for the atom, that is,

$$\rho(r) = \frac{1}{\frac{4}{3}\pi r_s^3}, \quad (26)$$

$$\rho(r) = \rho(r)_\uparrow + \rho(r)_\downarrow. \quad (27)$$

The last expression follows for helium since in the ground state the two electrons have opposite spin, but share the same spatial orbital. In this manner the correlation potential is included self-consistently and the density is obtained from the sum of the densities for each electron; that is, $\rho(r) = 2|\psi(r)|^2$. Finally, the correlation energy is obtained as

$$E_{\text{corr}} = \langle \psi_g | V_c(r) | \psi_g \rangle$$

and the value for the *total energy* is given by

$$E_{\text{total}} = E_{HF} + E_{\text{corr}}. \tag{28}$$

B. Density-functional theory

In the HF approximation, the many-body wave function is written in the form of a Slater determinant while the correlation energy is treated separately. This can be done for small systems, but for larger systems this is not an easy task. The theory of Kohn and Sham developed in 1965 simplifies both the exchange and correlation effect of electrons by reducing their effect to a effective potential V_{KS} that is *in principle* exact. In their seminal paper [49], they showed that to determine the ground state energy it is sufficient to determine the ground state electron density $\rho(r)$. By constructing a simple system of *noninteracting* electrons which yields the same density as the "real" fully interacting system, the ground state energy can be obtained.

The *Kohn-Sham equations* for two electrons are

$$\left[-\frac{1}{2}\nabla_1^2 - \frac{Z}{r_1} + \int d^3r_2 \frac{1}{|r_1 - r_2|}\rho(r_2) + V_{xc}(\rho) \right]\psi_i(r_1)$$
$$= \epsilon\psi_i(r_1). \tag{29}$$

These equations are self-consistent in the density and differ from the HF equations only in the exchange-correlation potential $V_{xc}[\rho]$ which is a function of the total local density, $\rho(r) = \sum_i^N |\psi_i(r)|^2$,

$$V_{xc}[\rho(r)] = \frac{\delta}{\delta\rho(r)}E_{xc}[\rho(r)]. \tag{30}$$

While the exact form of the exchange-correlation functional $E_{xc}[\rho]$ is not known, the simplest approximation is the local density approximation (LDA):

$$E_{xc}^{\text{LDA}}[\rho(r)] = E_x[\rho(r)] + E_c[\rho(r)], \tag{31}$$

$$E_x[\rho(r)] = -\left(\frac{3}{4}\right)\left(\frac{3}{\pi}\right)^{1/3}\int \rho(r)^{4/3}d^3r, \tag{32}$$

$$E_c[\rho(r)] = \int \frac{-0.29\rho(r)}{5.1 + r_s(r)}d^3r. \tag{33}$$

It follows from Eq. (30) that the potentials are given by

$$V_x[\rho(r)] = -\left(\frac{3}{\pi}\right)^{1/3}\rho(r)^{1/3}, \tag{34}$$

$$V_c[\rho(r)] = \frac{-0.29}{5.1 + r_s(r)} - \frac{1}{3}\frac{0.29r_s(r)}{[5.1 + r_s(r)]^2}, \tag{35}$$

and the ground state energy of the system is obtained from [44]

$$E_{\text{DFT}} = \sum_i^{N_e} \epsilon_i - \frac{1}{2}\iint d^3r_2 d^3r_1 \rho(r_1)\frac{1}{|r_1 - r_2|}\rho(r_2)$$
$$+ E_{xc}[\rho] - \int d^3r V_{xc}[\rho(r)]. \tag{36}$$

The Kohn-Sham equations are in general simpler than HF equations, while including correlation effects beyond the HF approximation. Furthermore, their computing time grows as a power of the number of the N electrons, whereas the exact solution for the N-electron Schrödinger equations is exponential in N [46].

Let us comment on the difference between the two approaches, even though both HF and Kohn-Sham equations have similar potential terms: $V_{\text{KIN}}, V_{en}, V_H, V_{xc}$ [see Eqs. (23) and (29)]. In HF the energy is calculated using the wave function explicitly, whereas in DFT the energy is a functional of the density. For example, for the correlation energy we have in the HF approximation

$$E_c^{HF} = \int |\psi(r)|^2 V_c(r) dr^3,$$

while for the DFT approximation we have

$$E_c^{\text{DFT}} = \int \rho(r)V_c[\rho(r)]dr^3.$$

Care should be exercised when computing the LDA exchange potential since this term is nonlinear in the density and as a result the normalization does not trivially cancel out when solving the eigenvalue problem. For example, in this work we use the normalization $\int |\psi(r)|^2 r^2 dr = 1$ so that a factor of $\sqrt{(4\pi)}$ is absorbed into the wave function $\psi(r) \rightarrow \psi(r)/\sqrt{(4\pi)}$. This, in turn, changes the density to $\rho = 2|\psi(r)|^2 \rightarrow 2\psi(r)^2/4\pi$, and therefore the exchange potential in LDA becomes

$$V_x[\rho(r)] = -\left(\frac{3}{\pi}\right)^{1/3}\rho(r)^{1/3} \rightarrow -\left(\frac{3\psi(r)^2}{2\pi^2}\right)^{1/3}.$$

In order to satisfy the boundary conditions $\psi(r) \rightarrow 0$ as $r \rightarrow \infty$, we use a uniform mesh with a cutoff radius at $r_{\text{cut}} = 10$ a.u. The radial equations where solved using C^0-continuous polynomials, that is, $N_{L \rightarrow R}(x) = x$ and $N_{L \leftarrow R}(x) = 1 - x$, where the function $N_{L \rightarrow R}(x)$ interpolates the wave function from the left node to the right node and similarly for $N_{L \leftarrow R}(x)$. We solved all the integrals numerically using 10-point Gaussian quadratures and in order to solve the generalized eigenvalue problem we have used a FORTRAN subroutine EWEVGE [52].

In Table I we show the energy components of the Kohn-Sham equations under LDA approximation and the HF equations using the Wigner correlation potential for the helium atom. We note that the reference values for the total energy (HF + Wigner correlation) are exact; therefore, even in the infinite basis limit the expression will not converge to the value shown. We also point out that the Perdue-Wang values on the correlation energy are obtained by using the random-phase approximation (RPA) for the free electron gas [51]. Our convergence value is limited by how well we can approximate this value. We have checked our level of convergence by

TABLE I. Comparison of various components to the Kohn-Sham and HF energies in hartrees for helium. The reference values (Perdue-Wang, Exact) are correct to all digits quoted [50,51], while the accuracy of the FEM estimates on E_{tot} is expected to be on the order of two digits (0.01) for $N = 100$ and three digits (0.003) for $N = 200$ for both LDA and total energy. Refer to the discussion on the text for details.

	LDA			Total energy		
	FEM ($N = 100$)	FEM ($N = 200$)	Perdue-Wang [50,51]	FEM ($N = 100$)	FEM ($N = 200$)	Exact [50]
$E_{tot} = E_{Kin} + E_{en} + E_H + E_{xc}$	−2.813 661	−2.821 852	−2.834 455	−2.886 297	−2.904 925	−2.903 724
E_{Kin}	2.703 352	2.726 064	2.767 389	2.806 848	2.855 856	2.867 082
E_{en}	−6.538 681	−6.571 185	−6.624 884	−6.664 319	−6.737 783	−6.753 267
E_H	1.973 543	1.978 456	1.995 861	1.020 329	1.026 754	1.024 568
E_x	−0.850 814	−0.854 086	−0.861 740	0.000 000	0.000 000	0.000 000
E_c	−0.101 061	−0.101 092	−0.111 080	−0.049 135	−0.049 814	−0.042 107
ϵ	−0.563 621	−0.565 805	−0.570 256	−0.957 555	−0.963 991	−0.903 724

increasing the number of elements to $N = 1000$ in a linear mesh of size $r_{cut} = 10$ a.u. with C^0-continuous basis (linear polynomials). We obtain a total energy of $E_{total}^{FEM} = -2.824\,596$ and correlation energy of $E_c^{FEM} = -0.101\,103$, and when compared to the values by Perdue-Wang (see Table I), the errors are $\delta E_{total} = 0.009\,859$ and $\delta E_c = 0.009\,977$, respectively. We see that the error in the total energy is dominated by the correlation term arising from using Wigner correlation rather than RPA description. However, taking this difference into account we can get an estimate for the error of all other terms, viz., $\delta E_{Kin} + \delta E_{en} + \delta E_H + \delta E_x \approx \delta E_{total} - \delta E_c = 0.000\,118$. In FEM, the error on L^2 integrals such as the energy is $O(h^{(p+1)})$, where h is the element width and p is the order of the polynomial used. Thus, for our example using $N = 1000$ in a uniform grid size with $r_{cut} = 10$ a.u. we have $h = 0.01$,

and since we employ a linear basis, the error we expect is $O(h^{(1+1)}) = 0.0001$. In this manner, if we take into account the intrinsic error due to the different energy-correlation terms we can recover the level of convergence expected by using FEM.

C. Exact formulation

We can compare the one-particle formalism above with an exact formulation of the system. In 1930 Breit showed that the Schrödinger equation for the two-electron atom becomes separable if one of the coordinate axes is aligned with one of the radius vector [53]. For the s state, the exact wave function depending on six total variables $\Psi(\vec{r}_1, \vec{r}_2)$ can be reduced to only three variables: the positions of the two electrons r_1 and r_2 and the angle between them θ_{12}, viz.,

$$\iiint \frac{1}{2} \frac{\partial \Psi^*}{\partial r_1} \frac{\partial \Psi}{\partial r_1} + \frac{1}{2} \frac{\partial \Psi^*}{\partial r_2} \frac{\partial \Psi}{\partial r_2} + \frac{1}{2} \left(\frac{1}{r_1^2} + \frac{1}{r_2^2} \right) \frac{\partial \Psi}{\partial \cos\theta_{12}} \frac{\partial \Psi}{\partial \cos\theta_{12}} + \Psi^* \left(-\frac{Z}{r_1} - \frac{Z}{r_1} + \frac{1}{r_{12}} - E \right) \Psi r_1^2 r_2^2 dr_1 dr_2 d\cos\theta_{12} = 0,$$

(37)

where

$$r_{12} = \sqrt{r_1^2 + r_2^2 - r_1 r_2 \cos\theta_{12}}.$$

We approximate the solution to the above Hamiltonian using FEM by discretizing each variable above independently as in Ref. [54]. The boundary conditions implemented make the wave function vanish at a cutoff radius of $r_{1,2} = 40$ a.u., and the angular range is between $-1 \leqslant \cos\theta_{12} \leqslant 1$. Furthermore, an adaptive grid was refined closer to the nuclei as shown in Fig. 1 to speed up calculations. In our implementation we use C^1-continuous basis, that is, Hermite polynomials $N_{L \to R}(x) = 1 - 3x^2 + 2x^3$ and $N_{L \leftarrow R}(x) = 3x^2 - 2x^3$, to interpolate the left and right nodal values of the wave function and additionally $\bar{N}_{L \to R}(x) = h_x(x - 2x^2 + x^3)$ and $\bar{N}_{L \leftarrow R}(x) = h_x(x^3 - x^2)$ to interpolate the derivatives of the wave function, where h_x is the element width and $x = \{r_1, r_2, \cos\theta_{12}\}$. In this manner, the continuity of the wave function is enforced by using this basis. All the integrals involved in constructing the matrices were

solved numerically using 10-point Gaussian quadratures, and in order to solve the generalized eigenvalue we used a sparse matrix solver in ARPACK++ [55].

For the mesh shown in Fig. 1, we obtain a ground state energy of $E_{exact}^0 = -2.7578$ using C^0-continuous basis and $E_{exact}^1 = -2.8994$ using C^1-continuous basis. The latter value is close to the energy obtained by Levin using the same approach $E^{(He)} = -2.9032$ [54], which is very close given that we perform all integrals numerically.

V. RESULTS AND DISCUSSION

In order to find the critical parameter we approximate the energy gap in the ground state numerically as

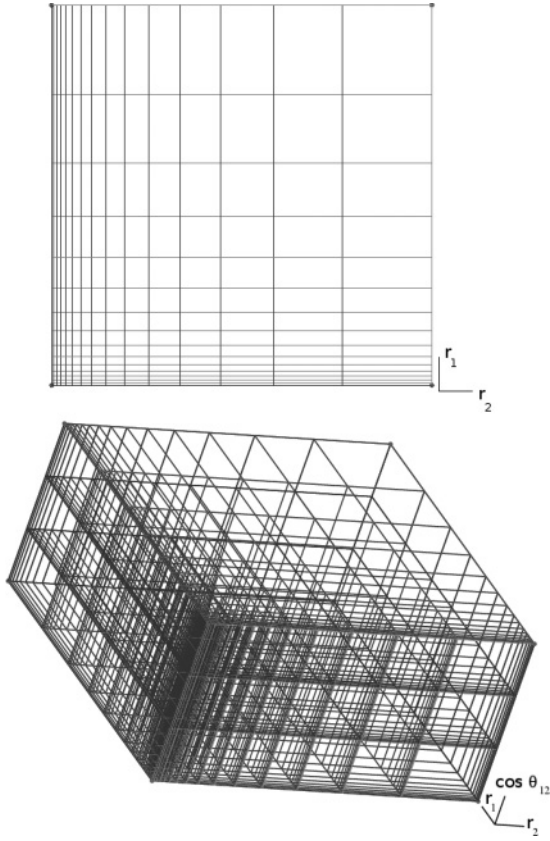$$\Delta E_0(Z) \approx E_0^{2e}(Z) - E_0^{(e)}(Z),$$

FIG. 1. Example of an adaptive mesh [56] used in approximating the solution in three dimensions. In this case the number of elements is $N_{\text{elements}} = 15 \times 15 \times 3 = 675$, while the size of the element progressively increases by a factor of 1.3 as $r_{1,2}$ is increased.

where $E_0^{(2e)}$ is the binding energy obtained for two electrons and $E_0^{(e)}$ is binding energy for a single electron. The theory of FSS is applied to a heliumlike Hamiltonian of the form

$$H = \underbrace{-\frac{1}{2}\nabla_1^2 - \frac{1}{2}\nabla_2^2 + \frac{1}{|r_1 - r_2|}}_{H_o} - \underbrace{\left(\frac{Z}{r_1} + \frac{Z}{r_2}\right)}_{V_Z}, \qquad (38)$$

where r_1 and r_2 are the coordinates of the two electrons referenced from the nuclei, and Z is the charge of the nucleus; this will play the role of the critical parameter. For reference, we note that the transformation $r \to r/Z$ takes Eq. (38) into

$$H(r \to r/Z)$$
$$= Z^2 \left[\underbrace{-\frac{1}{2}\nabla_1^2 - \frac{1}{2}\nabla_2^2 - \left(\frac{1}{r_1} + \frac{1}{r_2}\right)}_{H_o'} + \underbrace{\frac{1}{Z}\frac{1}{|r_1 - r_2|}}_{V_Z'} \right]; \qquad (39)$$

this form is often used in the literature to obtain the critical parameter $\lambda_c = 1/Z_c$ (see [42,43]). Below we outline a general procedure that can be used to combine FSS with numerical methods that expand a given wave function in the Hilbert space in any complete basis at a truncated level N.

A. General procedure

(1) Compute the expectation value of $\langle H \rangle^{(N)}$ and $\langle \frac{dH_Z}{dZ} \rangle^{(N)}$ for various values of N (number of elements). In this case the Hellmann-Feynman theorem [see Eq. (38)] becomes useful since in this case H_Z is linear in Z and the derivative is quite simple: $\langle \frac{dH_Z}{dZ} \rangle^{(N)} \to \langle \frac{dV_Z}{dZ} \rangle^{(N)}$.

(2) Construct the Γ function $\Gamma_\alpha(Z, N, N')$ [see Eq. (17)] for several values of (N, N') vs Z. At criticality, the Γ function $\Gamma_\alpha(Z, N, N')$ becomes independent of N and N' and the curves will cross. In Fig. 2 we show the Γ function we obtain by using different numbers of elements and how it begins to cross for various approximations to the energy.

(3) In order to go to the complete basis set limit $\langle H \rangle^\infty$, we have to let $(N, N') \to \infty$. The best choice is to keep $N - N'$ minimal [1,6]. Then, we proceed as follows: We solve $\langle H \rangle^{(N)}$ for $(N - 1, N, N + 1)$. This provides us with two Γ curves: $\Gamma_\alpha(Z, N - 1, N)$ and $\Gamma_\alpha(Z, N, N + 1)$, with minimum $N - N'$. The crossing of these two curves gives us the pseudocritical parameters $\alpha^{(N)}$ and $Z_c^{(N)}$ with a truncated basis set number N. Figure 3 illustrates the N dependence of the crossing.

(4) In order to extrapolate the values $\alpha^{(N)}$ and $Z_c^{(N)}$ to the infinite N limit, we use the algorithm of Burlish and Stoer [57]. Figures 4 and 5 show their behavior by systematically increasing N for the mean-field approximations and exact formulation, respectively.

While finding values $\alpha^{(N)}$ and $Z^{(N)}$ and extrapolating to the $1/N \to 0$ limit some numerical fluctuations can arise depending on the approximation used. We discuss some ways of dealing with these fluctuations. First, one can improve the basis used from C^0-continuous polynomials to C^1-continuous polynomials in order to obtain greater accuracy in the calculations; however, matrices double in size, increasing the memory cost as well as the computing time. Second, one can construct a Γ function from a potential in the Hamiltonian that explicitly takes into account all variables. For example, in the three-dimensional (3D) case we found that it is better to use the transformed Hamiltonian [Eq. (39)] where the perturbation V_λ is given by $V_{1/Z} = \frac{1/Z}{\sqrt{r_1^2 + r_2^2 - r_1 r_2 \cos\theta_{12}}}$ rather than $V_Z = \frac{Z}{r_1} + \frac{Z}{r_2}$. This does not change the physics of the system since both expressions can be used to find the critical value: either $1/Z_c$ or Z_c, which corresponds to one of the electrons going from a bound state into the continuum. The first perturbation $V_{1/Z}$ takes into account all three variables when the expectation value is computed, whereas the latter V_Z introduces numerical errors in the expectation value.

Last, another method is to increase the minimum difference $|N - N'| \geq \delta$ used in finding a crossing between $\Gamma_\alpha(Z, N - \delta, N)$ and $\Gamma_\alpha(Z, N, N + \delta)$ until a systematic crossing is obtained for all values of N; in the LDA approximations we used $|N - N'| = 5$, since the Γ curves change very little as the number of elements increases [see Fig. 2(c)], whereas in the 3D formulation we used $|\sqrt{N/3} - \sqrt{N'/3}| = 1$ since in this case the number of elements increases as $N_{\text{elements}} = N_{r_1} \times N_{r_2} \times N_{\cos\theta}$, and $N_{\cos\theta}$ was kept fixed at three. In solving the self-consistent equations [Eqs. (23) and (29)], we found that the region below $Z < 1$ became problematic when updating the self-consistent equations. This is because as the
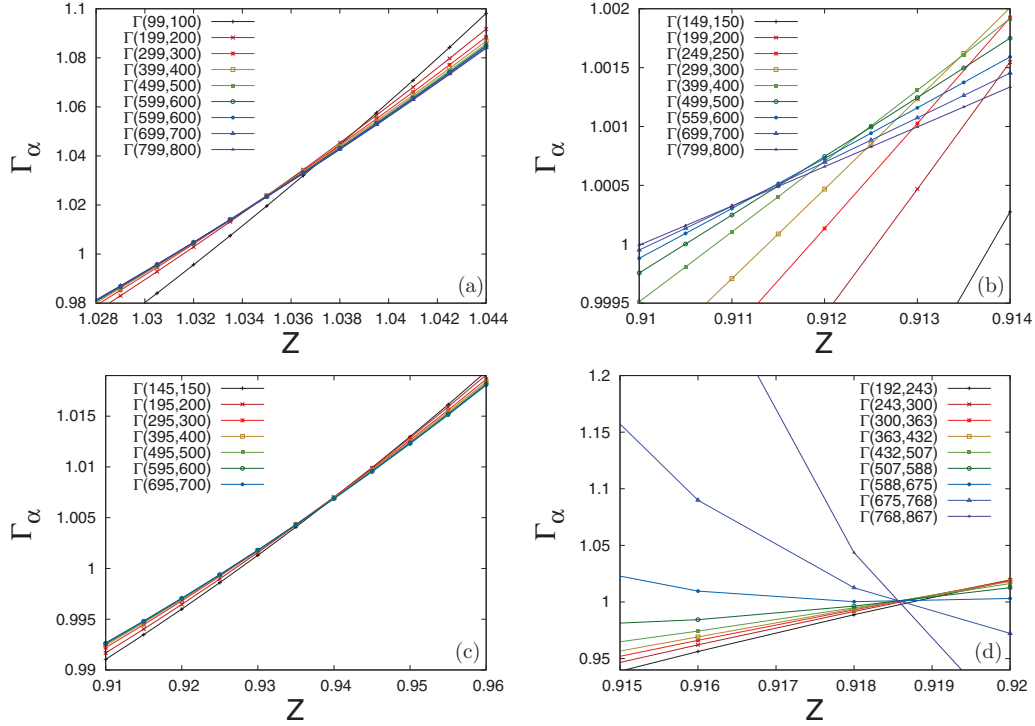
FIG. 2. (Color online) Plot of Γ_α [Eq. (17)] obtained by using FSS method as a function of the charge Z for increasing numbers of elements (N) for: (a) HF only, (b) total energy (HF + correlation energy), (c) LDA approximation, and (d) exact formulation.

nuclear charge decreases, the wave-function decay becomes slower with respect to r and the cutoff radius might lead to unphysical solutions (i.e., solutions which depend on r_{cut}). To get around this problem, we found it is useful to perturb the wave function with the arithmetic average of the current and predicted wave functions, rather than just the predicted wave function. In this manner, we can avoid converging to a local minima that corresponds to an unphysical solution.

In phase transition theory it is well known that using mean-field theory (for dimensionality $\leqslant 4$) does not give correct values near a critical point. This is indeed the case by using only the HF approximation (see Table II); however, we see that incorporating the exchange-correlation energy within the
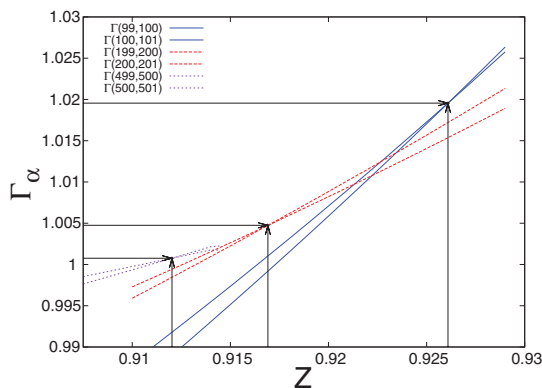

FIG. 3. (Color online) The crossing of $\Gamma_\alpha(Z, N - 1, N)$ and $\Gamma_\alpha(Z, N, N + 1)$ as N is increased using total energy approximation in HF. The crossing has been slightly enhanced in order to demonstrate the dependence of N.
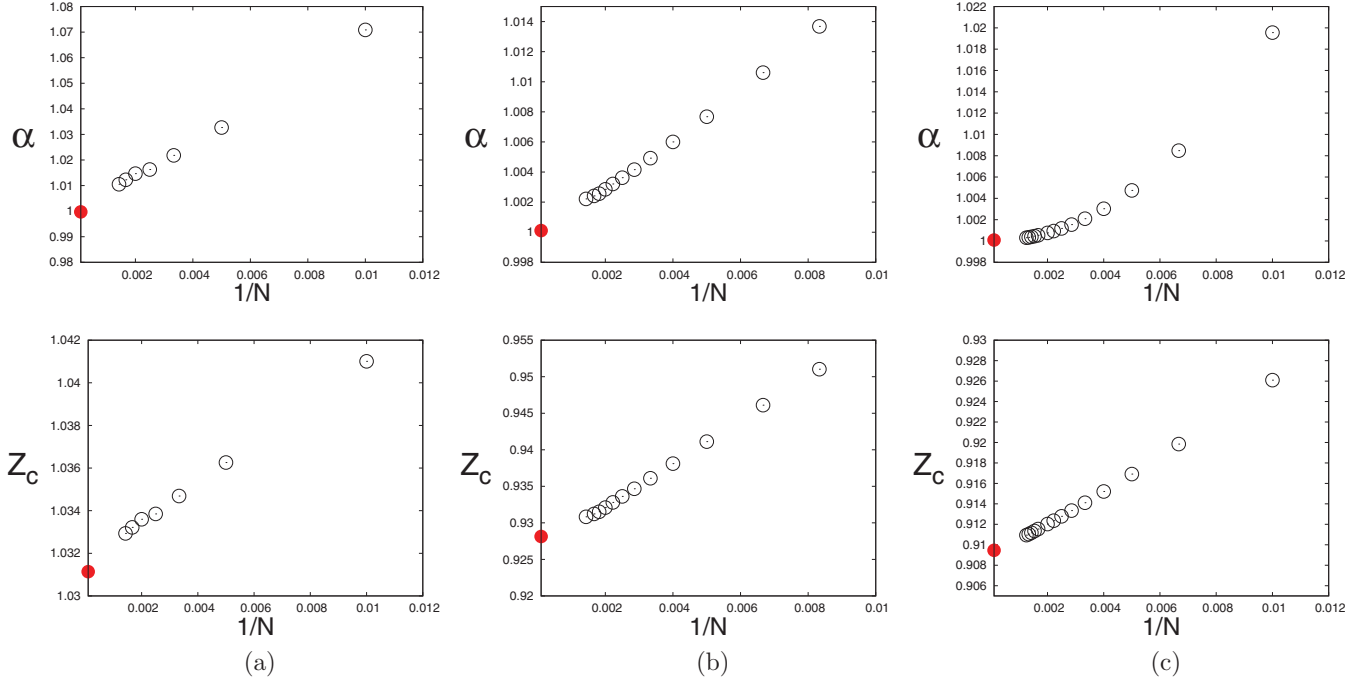
LDA approximation improves substantially the critical charge within 2% of the accepted value and within 1% using total energy approximation and exact formulation. It is interesting to note that all approaches give a consistent estimate for the critical exponent, regardless of the approximation used. This study demonstrates that FEM is a viable tool that can be applied in combination with FSS in order to obtain good estimates of critical parameters starting with *ab initio* calculations for electronic calculations such as DFT and HF and compare well with other methods that are deemed more precise.

We now check the consistency of our approach. In the theory of continuous phase transitions, a quantity diverging in the thermodynamic limit ($N \to \infty$), becomes a regular function for finite N, viz. $\langle O \rangle^{(N)} \sim N^{-\mu_o/\nu}$. We can check that this assumption is indeed satisfied for any value N. In the infinite basis limit we have the following form *near criticality*: $\langle O \rangle^{(\infty)} \sim (Z - Z_c)^{\mu_o}$ [Eq. (11)]. In this manner, can obtain the mth derivative of the energy near criticality given that we have a limiting expression for the energy, viz.,

$$E_Z \sim (Z - Z_c)^\alpha \Rightarrow \frac{d^m E_Z}{dZ^m} \sim (Z - Z_c)^{\alpha - m}. \quad (40)$$

In a finite basis the above expression becomes a power law in the number of basis with the following characteristic exponents:

$$E_Z^{(N)} \sim N^{-\alpha/\nu} \quad \text{and} \quad \frac{d^m E_Z^{(N)}}{dZ^m} \sim N^{-(\alpha - m)/\nu}. \quad (41)$$

FIG. 4. (Color online) Extrapolated values for the critical exponent α (top) and Z_c (bottom) for: (a) HF approximation, (b) LDA approximation, and (c) total energy. The filled dots are the extrapolated values for the $1/N \rightarrow 0$ limit.

Excluding the trivial case $N = 0$, one can therefore use Taylor expansion around $|Z - Z_c| \leqslant 1$:

$$E_Z^{(N)} = \sum_m \frac{d^m E_Z^{(N)}}{dZ^m} \frac{(Z - Z_c)^m}{m!} \qquad (42)$$

$$= \sum_m N^{(-\alpha+m)/\nu} \frac{(Z - Z_c)^m}{m!} \qquad (43)$$

$$= N^{-\alpha/\nu} \underbrace{\sum_m \frac{[N^{1/\nu}(Z - Z_c)]^m}{m!}} \qquad (44)$$

$$= N^{-\alpha/\nu} G_0[N^{1/\nu}(Z - Z_c)]. \qquad (45)$$

In this manner we obtain a universal scaling function G_0. Plotting $E^{(N)} N^{\alpha/\nu}$ vs the argument of the function G_0 would confirm whether the scaling function depends on N or not. Figure 6 shows that all quantities obtained from different N values do, in fact, collapse into one curve, and this confirms the scaling hypothesis for FSS with FEM [Eq. (10)]. In order to make the data collapse, it should be emphasized that the values α and Z_c used to produce Fig. 6 correspond to those obtained in Table II. If other values are used, the curves will *not collapse* and they will be distributed in a family of curves (N dependent) all deviating away from the unique curve shown in Fig. 6. The correlation length exponent was varied until the best collapse curve was found. This occurred around $\nu \approx 0.85 \pm 0.05$ for all implementations.
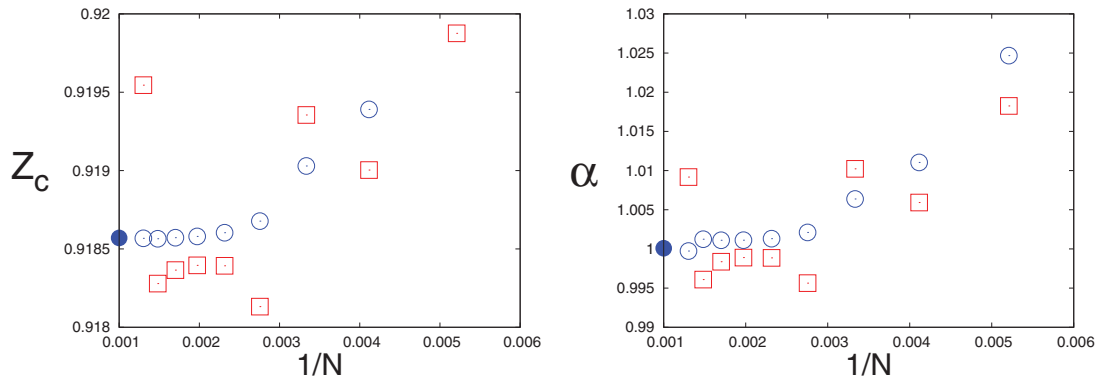

FIG. 5. (Color online) Extrapolated values for the critical exponent Z_c and α in the $1/N \rightarrow 0$ limit solving the system exactly in 3D. We construct the Γ_α function using *Hermite* interpolation polynomials for two potentials: $V_Z = -Z(\frac{1}{r_1} + \frac{1}{r_2})$ (denoted by □) and $V_Z = \frac{1/Z}{\sqrt{r_1^2 + r_2^2 - r_1 r_2 \cos\theta_{12}}}$ (denoted by ○); the latter is obtained by making the transformation $r \rightarrow r/Z$ in the Hamiltonian. We checked that the fluctuations seen in the figure vanish by replacing the numerical approximation to the binding energy with the analytical form, $E^{(e)} = Z^2/2$, while the extrapolated value remains unchanged.

TABLE II. Critical parameters extrapolated from Figs. 4 and 5.

	HF	LDA	Total Energy	Exact	References [10,43]
critical charge Z_c	1.031 14	0.928 08	0.909 46	0.918 57	0.911 03
critical exponent α	0.999 71	1.000 11	1.000 09	1.000 82	1.000 00

The solution to a set of HF or Kohn-Sham equations for large number of atoms becomes the limiting step, and it is here that the FEM can extend the range of sizes that can be investigated by other current means. The efficiency of FEM in the context of large-scale calculations derives from the strict locality of the FEM basis in real space, thus minimizing the need for extensive interprocessor communications on massively parallel computational architectures [14,20]. The work of Pask *et al.* [14,20] has formulated a real-space DFT approach for condensed matter applications without the need of using expensive Fourier transforms. Impressive results are obtained for GaAs calculations using this approach on DFT + FEM that systematically converges, as the number of elements is increased, to the values obtained using the conventional plane wave calculations, employing Fourier transforms and Ewald summations.

The scope of the dimension attainable with FEM has also been demonstrated by Sterne *et al.* [58]. They have employed FEM to compute positron distributions and lifetimes for various defect structures. Because the distribution is non-electron-like (concentrating away from the nuclei rather than around them), the generality of the FEM basis makes it particularly well suited for such problems. In order to study defects they have modeled a 5488 atom cell; as far as we know, this is one of the largest such calculations reported by any method to date.

Another applications of FEM to large-scale *ab initio* calculations is the work of Tsuchida *et al.* on molecular dynamics simulations of liquids [59]. They apply FEM study of liquid formamide (HCONH2) using a generalized gradient approximation to the exchange and correlation terms to improve the modeling of hydrogen bonds. The use of adaptive coordinate transformations helped to double the resolution of the basis at the C, N, and O centers. The liquid was modeled by 100 molecules in a cubic supercell of side 35.5 a.u., for a total of 600 atoms. The scope of this simulation is of the order of the largest one performed by standard PW methods to date and demonstrates the capacity of FEM for such large-scale computations already.

A new promising approach developed recently by Mazziotti [60] is the large-scale semidefinite programming for many-electron quantum mechanics. In this approach, the energy
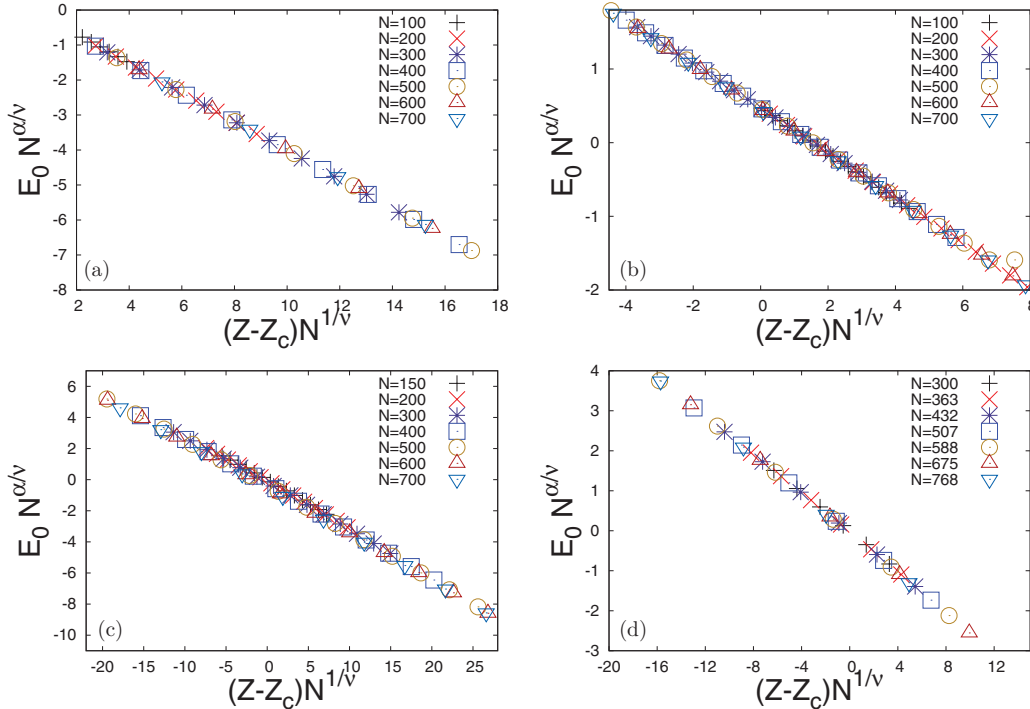

FIG. 6. (Color online) Data collapse for various values of N using: (a) HF, (b) total energy, (c) LDA approximation, and (d) exact formulation. The value from this collapse study that give us the best correlation length exponent $\nu \approx 0.85 \pm 0.05$, it should be emphasized that the values α and Z_c used in making these figures are the corresponding values for each approximation (i.e., those shown in Table II).

of a many-electron quantum system can be approximated by a constrained optimization of the two-electron reduced density matrix (2-RDM) that is solvable in polynomial time by semidefinite programming (SDP). The developed SDP method for computing strongly correlated 2-RDMs is 10–20 times faster than previous methods [61]. This approach was illustrated for metal-to-insulator transition of H_{50}, with about 10^7 variables.

These examples along with our current work, suggest that we can combine the FEM with FSS to obtain critical parameters in extended systems. One possibility is to calculate the phase transition at zero temperature in the 2D electron gas. The ground state energy of the system favors a crystallized state as the density of the electrons is lowered. Tanatar and Ceperey [62] performed a variational Monte Carlo simulation to the total energy using HF approach:

$$E_0(r_s) = E_{HF}(r_s) + E_c(r_s). \tag{46}$$

They find the gas-to-crystal transition at $r_s = 37 \pm 5$. This system would be ideal to test FEM with FSS for quantum criticality in extended systems.

VI. CONCLUSION

The theory of FSS has been demonstrated to be of great utility in analyzing numerical data of finite systems [1–8]. Moreover, it has been demonstrated that the theory also works for quantum systems, where the formalism applies to a complete basis expansion in the Hilbert space [24–33]. In this study we implemented the FEM which uses a local basis expansion consisting of arbitrary polynomials in real space and with variable resolution. It was demonstrated that this method can be used to compute matrix elements $\langle O \rangle^{(N)}$ (used in the FSS formalism) accurately and with monotonic convergence with respect to the system size N. We have implemented the combined approach on different approximations to electronic calculations such as HF approximation (+electron-electron correlation) and density-functional theory (DFT) under the LDA and found that even at the simplest level in DFT, the results we have obtained are in good agreement with other more accurate estimates such as large order perturbation theory [43].

The FEM has already shown great promise for extended systems since it uses local basis expansion to yield sparse matrices that lend the methodology easily to parallel architectures [14,19]. Furtermore, the Khon-Sham equations in DFT provide a general method for extended system. Therefore, we expect this combined approach can be applied to electron structure in atoms, molecules, and extended systems without loss of generality. Nevertheless, more studies need to be done to confirm the applicability of FSS with FEM for larger systems, where this combined approach can be used to shed some light into the nature of phase transitions.

[1] M. P. Nightingale, Physica A **83**, 561 (1976).

[2] J. L. Cardy, *Finite-Size Scaling* (Elsevier Science, New York, 1988).

[3] M. E. Fisher, in *Critical Phenomena*, Proceedings of the 51st Enrico Fermi Summer School, Verenna, Italy, edited by M. S. Green (Academic Press, New York, 1971); M. E. Fisher and M. N. Barber, Phys. Rev. Lett. **28**, 1516 (1972).

[4] B. Widom, in *Critical Phenomena in Fundamental Problems in Statistical Mechanics*, edited by E. G. D. Cohen (Elsevier, New York, 1975).

[5] M. N. Barber, in *Phase Transitions and Critical Phenomena*, edited by C. Domb and J. L. Labors (Academic Press, London, 1983), Vol. 8.

[6] V. Privman, *Finite Size Scaling and Numerical Simulations of Statistical Systems* (World Scientific, Singapore, 1990).

[7] P. J. Reynolds, H. E. Stanley, and W. Klein, J. Phys. A **11**, L199 (1978).

[8] P. J. Reynolds, H. E. Stanley, and W. Klein, Phys. Rev. B **21**, 1223 (1980).

[9] W. Moy, S. Kais, and P. Serra, Mol. Phys. **106**, 203 (2008).

[10] J. P. Neirotti, P. Serra, and S. Kais, Phys. Rev. Lett. **79**, 3142 (1997).

[11] E. Antillon, W. Moy, Q. Wei, and S. Kais, J. Chem. Phys. **131**, 104105 (2009).

[12] E. Tsuchida and M. Tsukada, Phys. Rev. B **54**, 7602 (1996).

[13] D. Stiles (private communication).

[14] J. E. Pask and P. A. Sterne, Modell. Simul. Mater. Sci. Eng. **13**, R71 (2005).

[15] L. R. Ram-Mohan, *Finite Element and Boundary Element Applications in Quantum Mechanics* (Oxford University Press, London, 2002).

[16] D. W. Pepper and J. C. Heinrich, *The Finite Element Method* (Taylor & Francis, New York, 2006).

[17] O. Taisuke and T. Masayuki, Comput. Phys. Commun. **182**, 1245 (2011).

[18] J. E. Bylaska, M. Holst, and J. H. Weare, J. Chem. Theor. Comp. **5**, 937 (2009).

[19] R. Alizadegan, K. J. Hit, and T. J. Martinez, J. Chem. Phys. **132**, 034101 (2010).

[20] J. E. Pask, B. M. Klein, C. Y. Fong, and P. A. Sterne, Phys. Rev. B **59**, 12352 (1999).

[21] C. N. Yang and T. D. Lee, Phys. Rev. **87**, 404 (1952).

[22] T. D. Lee and C. N. Yang, Phys. Rev. **87**, 410 (1952).

[23] S. Sachdev, *Quantum Phase Transitions* (Cambridge University Press, Cambridge, 1999).

[24] J. P. Neirotti, P. Serra, and S. Kais, Phys. Rev. Lett. **79**, 3142 (1997).

[25] P. Serra, J. P. Neirotti, and S. Kais, Phys. Rev. Lett. **80**, 5293 (1998).

[26] S. Kais, J. P. Neirotti, and P. Serra, Int. J. Mass Spectrom. **182**, 23 (1999).

[27] P. Serra, J. P. Neirotti, and S. Kais, Phys. Rev. A **57**, R1481 (1998).

[28] P. Serra, J. P. Neirotti, and S. Kais, J. Phys. Chem. A **102**, 9518 (1998).

[29] J. P. Neirotti, P. Serra, and S. Kais, J. Chem. Phys. **108**, 2765 (1998).

[30] Q. Shi and S. Kais, Mol. Phys. **98**, 1485 (2000).

[31] S. Kais and Q. Shi, Phys. Rev. A **62**, 060502 (2000).

[32] S. Kais and P. Serra, Int. Rev. Phys. Chem. **19**, 97 (2000).

[33] S. Kais and P. Serra, Adv. Chem. Phys. **125**, 1 (2003).

[34] P. Serra and S. Kais, Chem. Phys. Lett. **372**, 205 (2003).

[35] A. Ferron, P. Serra, and S. Kais, J. Chem. Phys. **120**, 8412 (2004).

[36] Q. Shi and S. Kais, Mol. Phys. **98**, 1485 (2000).

[37] Q. Shi and S. Kais, Int. J. Quantum Chem. **85**, 307 (2001).

[38] A. Ferron, P. Serra, and S. Kais, J. Chem. Phys. **128**, 044307 (2008).

[39] B. Simon, J. Funct. Anal. **25**, 338 (1977).

[40] L. D. Landau and E. M. Lifshitz, *Quantum Mechanics: Non-relativistic Theory*, Vol. 3, 3rd ed. (Butterworth-Heinemann, London, 1981).

[41] S. Chandrasekhar, Astrophys. J. **100**, 176 (1944).

[42] F. H. Stillinger and D. K. Stillinger, Phys. Rev. A **10**, 1109 (1974).

[43] J. D. Baker, D. E. Freund, R. N. Hill, and J. D. Morgan III, Phys. Rev. A **41**, 1247 (1990).

[44] J. M. Thijssen, *Computational Physics* (Cambridge University Press, Cambridge, 1999).

[45] W. Schweizer. *Numerical Quantum Dynamics* (Kluwer Academic Publishers, Dordrecht, 2001).

[46] G. Giuliani and G. Vignale, *Quantum Theory of the Electron Liquid* (Cambridge University Press, Cambridge, 2005).

[47] H. Mitler, Phys. Rev. **99**, 1835 (1955).

[48] C. W. Ufford and J. G. Thomas, Phys. Rev. **133**, A121 (1964).

[49] W. Kohn and L. Sham, Phys. Rev. A **140**, 1133 (1965).

[50] C. J. Umrigar and X. Gonze, Phys. Rev. A **50**, 3827 (1994).

[51] J. P. Perdew and Y. Wang, Phys. Rev. B **45**, 13244 (1992).

[52] D. Porezag, [http://beam.acclab.helsinki.fi/~akrashen/escalc/mathsub.f].

[53] G. Breit, Phys. Rev. **35**, 569 (1930).

[54] F. S. Levin and J. Shertzer, Phys. Rev. A **32**, 3285 (1985).

[55] F. M. Gomes, [http://www.ime.unicamp.br/~chico/arpack++].

[56] C. Geuzaine and J. Remacle, [http://geuz.org/gmsh/].

[57] R. Bulirsch and J. Stoer, Num. Math **6**, 413 (1964).

[58] P. A. Sterne, J. E. Pask, and B. M. Klein, Appl. Surf. Sci. **149**, 238 (1999).

[59] E. Tsuchida, J. Chem. Phys. **121**, 4740 (2004).

[60] D. A. Mazziotti, Phys. Rev. Lett. **106**, 083001 (2011).

[61] D. A. Mazziotti, Phys. Rev. Lett. **93**, 213001 (2004).

[62] B. Tanatar and D. M. Ceperley, Phys. Rev. B **39**, 5005 (1989).